Green Emulating Energetic Viable Alternate Fuel (GEEVA Fuel)

ANANTHALAKSHMI S[1], PROF. DR. SANKARAN A[2], SUDHANSHU SRIVASTAVA[3]
[1, 3] M E Aeronautical Engineering, Nehru Institute of Engineering and Technology, Coimbatore.
[2] Professor, Dept. of Aeronautical Engineering, Nehru Institute of Engineering and Technology, Coimbatore.

Abstract—Green propellants are high energy liquid rocket propellants that operate as a high-performance, high-efficiency alternative to conventional chemical propellants for future spacecraft. Green propellants are attractive as possible substitutes for traditional hazardous propellants. This research is targeted at green propellants that are the most viable for rocket or spacecraft propulsion. The term viability is based on the features such as less pollution, maximum efficiency, ease of transportation and handling. Thus, this paper aims to analyze a propellant module as a possible green propellant for rocket propulsion that combines the best of worlds that is, safety and efficiency. The analysis is done using the Analytical Systems (ANSYS 2021 R1) software package, particularly the fluent analysis system.

Indexed Terms— combustion temperature, efficiency, green propellants, specific impulse.

I. INTRODUCTION

Rocket engines employ the principle of jet propulsion. The rocket engines powering rockets come in a great variety of different types. Most current rockets are chemically powered rockets (usually internal combustion engines, but some employ a decomposing monopropellant) that emit a hot exhaust gas. A rocket engine can use gas propellants, solid propellant, liquid propellant, or a hybrid mixture of both solid and liquid. Some rockets use heat or pressure that is supplied from a source other than the chemical reaction of propellant(s), such as steam rockets, solar thermal rockets, nuclear thermal rocket engines or simple pressurized rockets such as water rocket or cold gas thrusters. With combustive propellants a chemical reaction is initiated between the fuel and the oxidizer in the combustion chamber, and the resultant hot gases accelerate out of the rocket engine nozzle (or nozzles) at the rearward-facing end of the rocket. The acceleration of these gases through the engine exerts force ("thrust") on the combustion chamber and nozzle, propelling the vehicle (according to Newton's Third Law). This actually happens because the force (pressure times area) on the combustion chamber wall is unbalanced by the nozzle opening; this is not the case in any other direction. The shape of the nozzle also generates force by directing the exhaust gas along the axis of the rocket. The reaction mechanisms are investigated for combustion of the various propellant modules. It is clear that the phenomenology of silane combustion is different than that for hydrocarbon combustion. Some of the unusual behavior include the following: Silane mixtures are characterized by very low self-ignition temperatures. Autoignition can occur at room or even lower temperatures. The lower and upper limits of chain ignition are observed experimentally at low pressures. Most data indicate the chain-branching nature of ignition at room temperature and 1 bar. The analysis of the propellant modules is done in ANSYS 2022 R1 Fluent module. The temperature and velocity of the resultant gases on combustion are recorded. The specific impulse is calculated as a parameter for comparison of fuel efficiency.

II. METHODOLOGY

A. Details of Geometry

The combustion chamber and nozzle geometry were made using the geometry design Modeler in ANSYS 2022 R1 software, using the dimensions below in Fig.2.1.

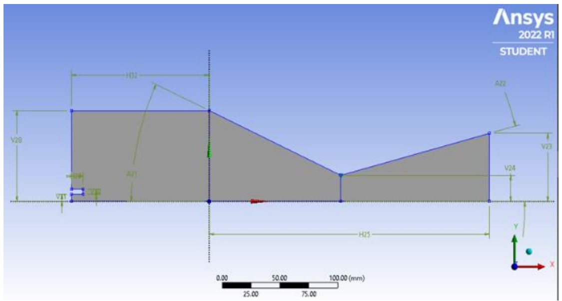

Fig. 2.1: Geometry

The dimensions of the created sketch are indicated in Table 2.1:

Table 2.1: Sketch dimensions

Sketch component	Dimensions
A21	25°
A22	15°
H25	242.29 mm
H29	10 mm
H32	119.1 mm
V23	55.753 mm
V24	21. 336 mm
V28	74.422 mm
V30	4mm
V31	6mm

B. Details of Meshing

The meshing of the model is done in ANSYS 2022 R1 Meshing module. A structured quadrilateral mesh is generated. Appropriate edge sizing is given to all the edges of the geometry. The number of nodes and elements formed are 5355 and 5046 respectively. The mesh settings are similar for both the viscous models to compare the results. Face sizing is applied to all the faces to obtain a structured mesh.

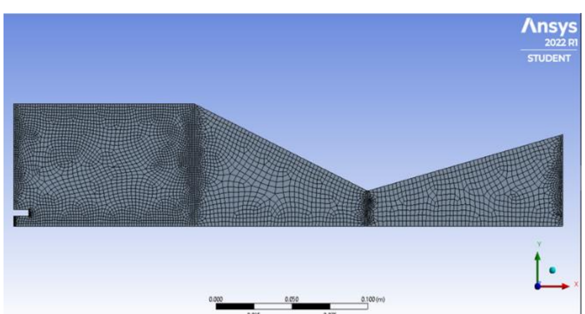

Fig. 2.2: Meshing of the model

The mesh is refined and corrected for fineness so that the computational accuracy and time trade-off is minimum.

C. Details of Setup

- Setup: In setup, double precision with parallel processing option is selected with number of processes set to 4.

- General: The scale is adjusted to appropriate levels. solver type is set to pressure-based to calculate the compressible effects of the fluid through chamber. Swirl effects are enabled. The flow is symmetric about X axis so 2-D space is set to axisymmetric. Gravity effects are neglected.

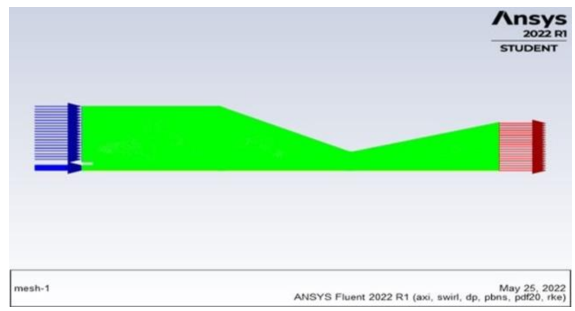

Fig. 2.3: Scaled mesh

- Models: The energy equation is turned ON for all the flow analysis. For Ideal flow conditions the viscous model is set to Inviscid. To simulate a turbulent flow k-ϵ (standard) viscous model is used.

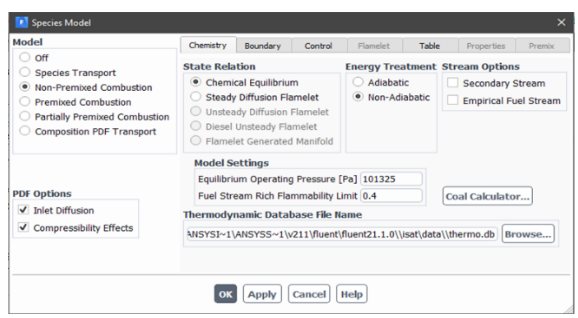

Fig. 2.4: Non-Premixed combustion setup

To facilitate combustion of the target materials listed in the table below, we select non-premixed combustion with settings as shown in Fig. 2.4.

The various propellant combinations used are shown in Table 2.2

Table 2.2: Propellant modules

Propellant module number	Propellant module
1	Silane (SiH_4)-Oxygen (O_2)-Nitrogen (N_2)
2	Silane (SiH_4)-Hydrogen (H_2)-Oxygen (O_2)

We set the mass fractions of fuel and oxidizer for a dimensionless analysis, irrespective of the actual amount of fuel used, as shown in the table 2.3 below.

Table 2.3: Fuel species mass fractions

Sl. No .	Fuel module	Fuel combination in moles
1	SiH_4-O_2-N_2	SiH_4: 0.02; N_2: 0.86; H_2: 0.08; O_2: 0.04; O_2:1
2	SiH_4-H_2-O_2	SiH_4: 0.02; H_2: 0.98; O_2: 1; O_2: 0.04
3	SiH4-HNO3-N2-H2-O2	N_2: 0.86; O_2: 1; NH_3: 0.05; HNO_3: 0.07; SiH_4: 0.02;

- Boundary conditions: We set the boundary conditions at the boundary zones as shown in Fig. 2.5. Air inlet was given velocity of 0.6m/s, whereas the fuel injection velocity was set as 82 m/s. The turbulent intensity and turbulent viscosity ratio were set as 10% and 10 respectively. The symmetrical axis was set as axis.

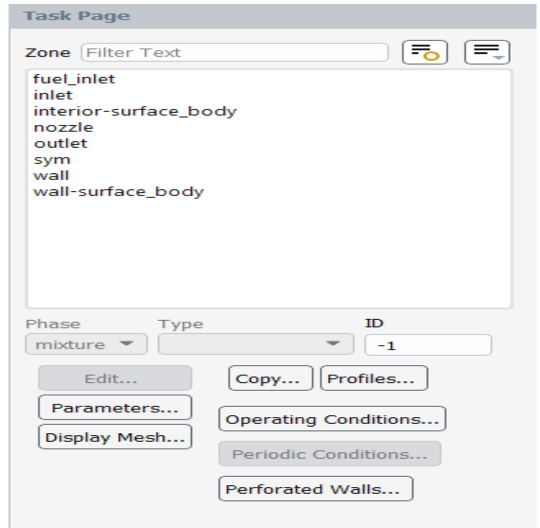

Fig.2.5: Boundary zones

The nozzle wall is set as bounded by temperature conditions, as shown in Fig.2.6.

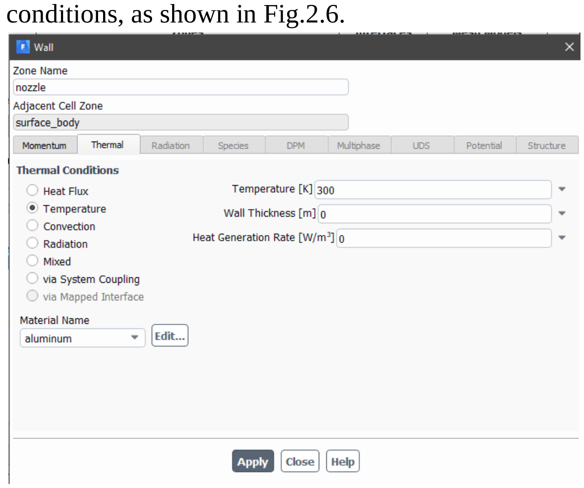

Fig. 2.6: Nozzle wall boundary conditions

- Reference values: The simulation was set to compute from inlet and reference zone was given as surface body. The following figure (Fig. 2.7) shows the values that were entered for the analysis.

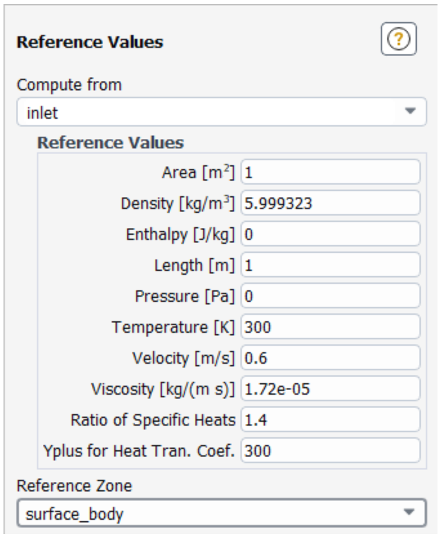

Fig.2.7: Reference values

- Solution Methods: The scheme followed for solution is coupled and spatial discretization gradient is least squares cell based. The remaining settings are default. All solver methods except Turbulent kinetic energy are set to second order discretization for maximum accuracy, as shown in Fig. 2.8.

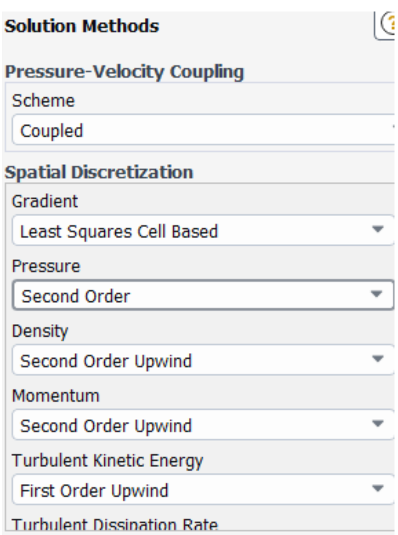

Fig. 2.8: Solution Methods

Solution controls: The default settings are followed at this stage.

Initialization methods: Hybrid initialization is followed for the solution initialization.

Run calculation: The number of iterations is given as 1000. The remaining settings are followed as the default settings.

III. RESULTS AND DISCUSSION

The simulation of flow is carried out under steady state condition. Contours of temperature and velocity are obtained. The average values of the parameters at the chamber exit plane are noted down. In this section the variations in pressure, temperature and velocity of fluid and oxidizer for inviscid and k-ϵ viscous model are discussed and compared to theoretical values obtained.

A. Temperature

The contours of static temperature are obtained for each of the propellant combinations, and are presented below.

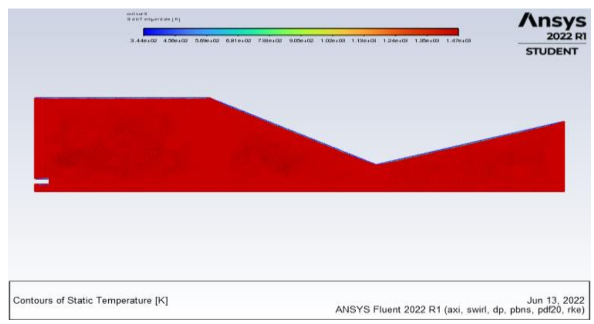

Fig. 3.1: Contours of static temperature of Si-O2

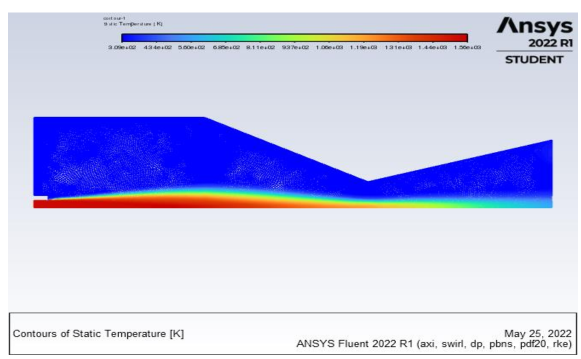

Fig. 3.2: Contours of static temperature on combustion of Si-H2-O2

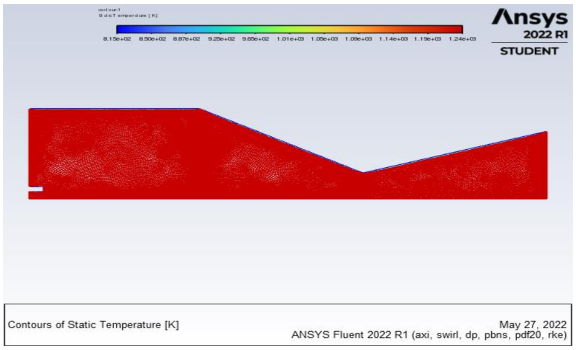

Fig. 3.3: Contours of static temperature on combustion of SiH4-HNO3-N2-H2-O2

Results obtained for maximum temperature resulting on propellant combustion is given in Table 3.1.

B. Pressure

The contours of static pressure are obtained for each of the propellant combinations, and are presented below.

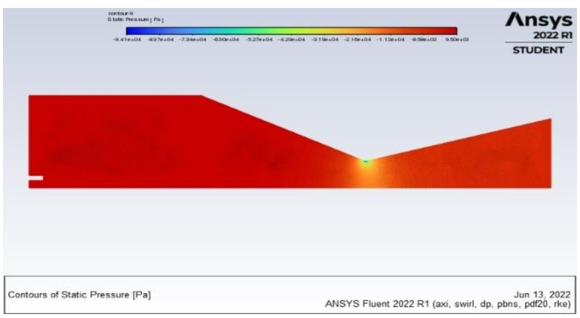

Fig. 3.4: Contours of static pressure obtained on combustion of Si-O_2

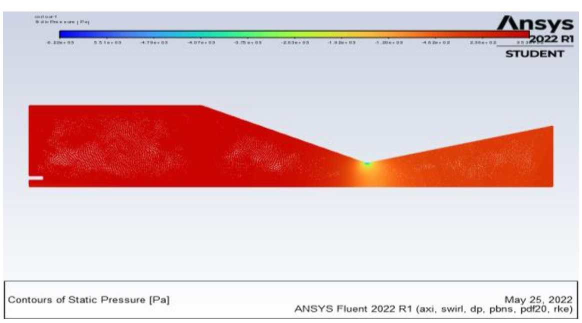

Fig. 3.5: Contours of static pressure obtained on combustion of Si-H_2-O_2

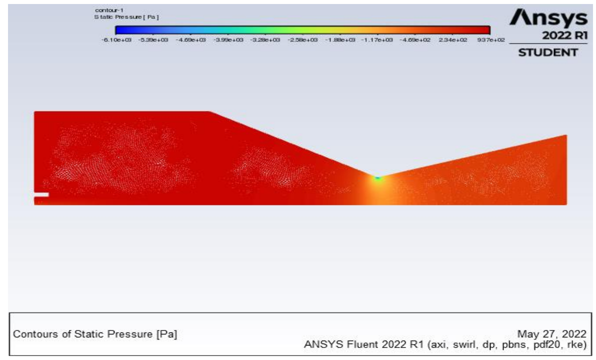

Fig.3.6: Contours of static pressure obtained on combustion of SiH4-HNO3-N2-H2-O2

Results obtained for maximum pressure resulting on propellant combustion is given in Table 3.1.

C. Velocity

The contours of velocity are obtained for each of the propellant combinations, and are presented below.

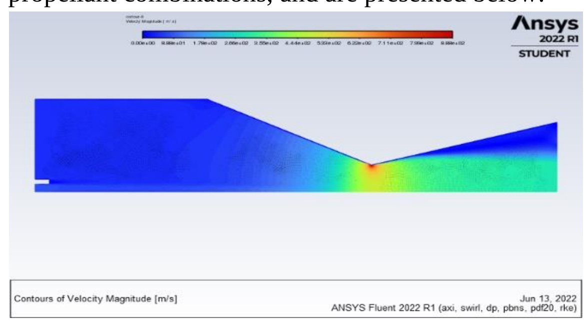

Fig. 3.7: Contours of velocity obtained on combustion of Si-O2

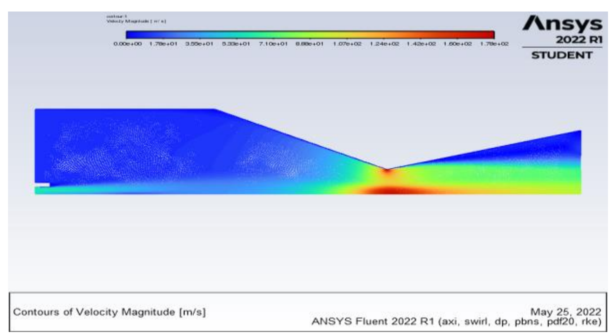

Fig. 3.8: Contours of velocity obtained on combustion of Si-H2-O2

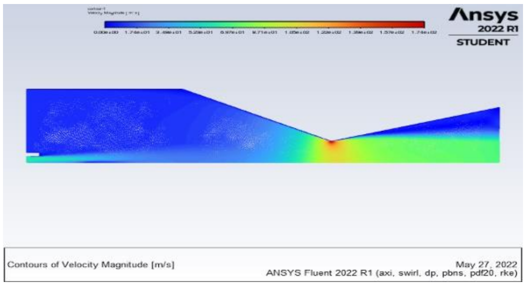

Fig. 3.9: Contours of velocity obtained on combustion of SiH4-HNO3-N2-H2-O2

The specific impulse (Isp) values are usually calculated using either of the following formulae:

$$Isp = \frac{V}{g} \qquad \dots (1)$$

Where
Isp: Specific impuulse in seconds (s)
V: Velocity in m/s
g: Acceleration due to gravity in m/s

$$Isp = \frac{F}{\dot{m}g} \qquad \dots (2)$$

Where
Isp: Specific impulse in seconds (s)
F: Thrust in newton (N)
ṁ: Mass flow rate in kg/s
g: Acceleration due to gravity in m/s

However, in this case, the specific impulse is calculated using an open-source code [1].

The values of specific impulse obtained in the analysis is less than that of conventional values of specific impulse required for rocket propulsion, because the testing is done in gaseous phase, and thus the density is less than that of the cryogenic liquid phase propellants used in the rocket propellants.

From the results, the fuel module 1 (SiH_4-O_2-N_2) gives the best values of Specific impulse compared to the other two fuel modules. It is inferred that the presence of the other components like nitrogen, hydrogen and nitric acid reduces the energy output of the propellent combination.

Table: 3.1: Fuel Modules and their Static Pressure, Static Temperature and Specific impulse (Isp)

S. No.	Fuel Module	Static Pressure (Pa)	Static Temperature (K)	Specific Impulse (Isp) (s)
1	SiH_4-O_2-N_2	11368.47	1484.486	92.5
2	SiH_4-H_2-O_2	10911.81	1699.766	93.23
3	SiH_4-HNO_3-N_2-H_2-O_2	13205.06	1125.195	92.6

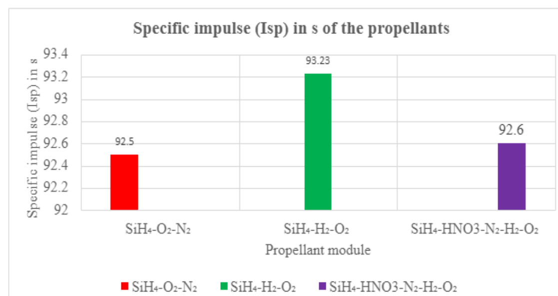

Fig. 3.10: Comparison of resultant specific impulse of various propellant modules

Reaction mechanism of the first fuel module is shown in Table 3.2

Table 3.2: Reaction mechanism of SiH_4-O_2 fuel module [2]:

No.	Reaction	A	nf	Ef
R1	H2O + M = H+OH + M	2.20E+16	0.0	1.050E+05
R2	HO2 + M = H+O2+ M	2.31E+15	0.0	4.590E+04
R3	OH + M = O+ H + M	8.00E+19	-1.0	1.037E+05
R4	O2 + M = O+O+ M	5.10E+15	0.0	1.150E+05

R5	H2 + M = H+H+M	2.20E+14	0.0	9.600E+04
R6	O2+H2 = OH+OH	8.00E+14	0.0	4.500E+04
R7	HO2+O = O2+OH	5.00E+13	0.0	1.000E+03
R8	H+O2 = O+OH	2.20E+14	0.0	1.679E+04
R9	H2+O = H+OH	1.80E+10	1.0	8.900E+03
R10	O+H2O = OH+OH	6.80E+13	0.0	1.835E+04
R11	H+H2O = OH+H2	9.50E+13	0.0	2.030E+04
R12	HO2 + M = O+OH + M	8.18E+21	-1.0	6.585E+04
R13	SIH4+OH = SIH3+H2O	8.70E+12	0.0	9.500E+01
R14	SIH4+O = SIH3+OH	4.00E+12	0.0	1.580E+03
R15	SIH4+HO2 = SIH3+H2O2	2.00E+12	0.0	1.000E+04
R16	XSIH3O2 = SIH3+O2	3.66E+20	-1.0	7.160E+04
R17	H+HO2 = OH+OH	2.50E+14	0.0	1.900E+03
R18	H+HO2 = H2+O2	2.50E+13	0.0	7.000E+02
R19	OH+HO2 = H2O+O2	5.00E+13	0.0	1.000E+03
R20	H2O2+O2 = HO2+HO2	4.00E+13	0.0	4.264E+04
R21	H2O2 + M = OH+OH + M	1.20E+17	0.0	4.550E+04
R22	HO2+H2 = H2O2+H	7.30E+11	0.0	1.870E+04
R23	SIH2+O2 = HSIO + OH	1.00E+14	0.0	3.700E+03
R24	SIH2O+H = HSIO+H2	3.30E+14	0.0	1.050E+04
R25	SIH2O+HO2 = HSIO+H2O2	1.00E+12	0.0	8.000E+03
R26	SIH4 = SIH2+H2	5.00E+12	0.0	5.220E+04
R27	SIH4 = SIH3+H	3.69E+15	0.0	9.300E+04
R28	HSIO + M = H+SIO + M	5.00E+14	0.0	2.900E+04
R29	HSIO+H = SIO+H2	2.00E+14	0.0	0
R30	HSIO+O = SIO+OH	1.00E+14	0.0	0
R31	HSIO+OH = SIO+H2O	1.00E+14	0.0	0
R32	HSIO+O2 = SIO+HO2	3.00E+12	0.0	0
R33	SIO+O2 = SIO2+O	1.00E+13	0.0	6.500E+03
R34	SIO+OH = SIO2+H	4.00E+12	0.0	5.700E+03
R35	SIO2 + M = SIO+O	0	0.0	0

	+ M			
R36	SIH3O2 = SIH2O+OH	8.60E+14	0.0	4.000E+04
R37	SIH3+H2=SIH2O+O	7.60E+13	0.0	4.40E+04
R38	SIH2O+O = HSIO+OH	1.80E+13	0.0	3.08E+03
R39	SIH4+SIH3O = SIH3+SIH3OH	2.00E+11	0.0	5.30E+03
R40	SIH4+SIH3O2 = SIH3+SIH3O2H	L.10E+13	0.0	L.85E+04
R41	SIH3O2+SIH2O = SIH3O2H+HSIO	L.30E+11	0.0	6.80E+03
R42	SIH3O2+HO2 = SIH3O2H+O2	4.00E+10	0.0	0
R43	SIH3O2H = SIH3O+OH	6.50E+14	0.0	4.870E+04
R44	SIH3O2H+H = SIH3O2+H2	4.80E+13	0.0	7.950E+03
R45	SIH3O+SIH2O = SIH3OH+HSIO	1.20E+11	0.0	9.710E+02
R46	SIH3O + SIH3OH=SIH3OH + SIH2OH	L.50E+12	0.0	5.300E+03
R47	SIH3O+O2 = SIH2O+HO2	1.00E+12	0.0	4.50E+03
R48	SIH3OH+H = SIH2OH+H2	3.00E+13	0.0	5.30E+03
R49	SIH3OH+O = SIH2OH+OH	L.70E+12	0.0	L.73E+03
R50	SIH3OH+OH = SIH2OH+H2O	4.00E+12	0.0	L.50E+03
R51	SIH3OH+SIH3 = SIH2OH+SIH4	1.80E+11	0.0	7.40E+03
R52	SIH3OH +SIH3O2=SIH2OH +SIH3O2H	6.300E+12	0.0	L.450E+04
R53	SIH3OH+O2 = SIH2OH+HO2	4.00E+13	0.0	4.50E+04
R54	SIH3OH+HO2 = SIH2OH+H2O2	6.30E+12	0.0	L.40E+04
R55	SIH2O+O2 = HSIO+HO2	4.00E+14	0.0	2.95E+04
R56	SIH2OH +O2 = HSIOOH + OH	L.00E+13	0.0	7.00E+03

R57	HSIO+SIH3O = SIO+SIH3OH	1.00E+12	0.0	0
R58	XSIH3O2 = SIH3O+O	1.76E+08	0.0	0
R59	XSIH3O2 = SIH2O+OH	3.00E+12	0.0	6.33E+03
R60	XSIH3O2 = HSIOOH + H	1.14E+08	0.0	0
R61	SIH2O + H2O = HSIOOH + H2	1.00E+13	0.0	0
R62	SIH2O + OH = HSIOOH + H	L.00E+13	0.0	0
R63	SIH2O + HO2 = HSIOOH + OH	1.00E+11	0.0	0
R64	HSIOOH + O2 = SIOOH + HO2	1.70E+13	0.0	L.60E+04
R65	HSIOOH = SIOOH+H	5.00E+14	0.0	6.50E+04
R66	SIOOH+O2 = SIO2+HO2	1.00E+12	0.0	1.43E+04
R67	XSIH3O2 + M = SIH3O2 + M	1.17E+13	0.0	0
R68	SIOOH = SIO2 + H	4.00E+15	0.0	4.00E+15
R69	SIOOH + H = SIO2 + H2	1.00E+12	0.0	1.00E+12

From the reactions through 1 to 69, we can observe the various stages of reaction and the species involved. There are no pollutant species throughout other than SiO2 which forms a residue film and H2O2. This proves that the best fuel module is SiO2 which also is also non-polluting and clean.

CONCLUSION

Three propellant modules namely SiH_4-O_2-N_2, SiH_4-H_2-O_2 and SiH_4-HNO3-O_2-N_2 are analysed in this paper. The first module, i.e., SiH_4-O_2-N_2 is found to have the highest combustion temperature and is non-polluting as inferred from the reaction mechanism. The possibility of formation of silicon residues is predicted. The decrease in reaction rate also indicates the decrease in pollution in the exhaust stream as well as the ambient. Thus, the propellant combination SiH_4-O_2-N_2 can be proposed as a green propellant for use in rocket propulsion.

ACKNOWLEDGMENT

We are thankful to our parents, Gurus and the sustaining powers of the Universe for always being by our side and providing us with the strength and capability to prove ourself to everyone. We are very much grateful to beloved Founder Chairman of Nehru Group of Institutions, Late. Shri. P.K. DAS, for giving us an opportunity to study in this wonderful institution and for the various excellent facilities to learn, develop and excel ourselves in various fields. We would like to share our thanks to the Chairman and Managing Trustee Adv. Dr. P. KRISHNA DAS for favouring us to do the project and offering the adequate infrastructure and amenities for completing our project. We thank our respected CEO & SECRETARY Dr. P. KRISHNAKUMAR, Nehru Group of Institutions, Coimbatore for providing the facilities. We would like to thank the Management of the college and the honourable principal Dr. P.

MANIARASAN. M.E., Ph.D., for providing support in this venture.

Our sincere thanks to the Director Prof. Dr. A. SANKARAN, M.E., Ph.D., who supported us as an excellent guide and mentor of our project. His meticulous counsel and grace helped us to successfully complete our project. We would like to sincerely thank Prof. Dr. B. R. SENTHIL KUMAR, M.E., Ph.D., Head of the Department of Aeronautical Engineering, for his encouragement and consistent advice during the course of this project.

We are thankful to our Project Coordinator Mr. R. KOUSIK KUMAAR, MTech, (PhD)., Assistant Professor, Department of Aeronautical Engineering for providing the adequate guidance and for his valuable comments and suggestions.

We are very grateful to our project supervisor Prof. Dr. A. SANKARAN for directing us through the right path to gain more knowledge.

REFERENCES

[1] https://www.omnicalculator.com/physics/specific-impulse

[2] E.L. Petersen, D.M. Kalitan, M.J.A. Rickard, M.W. Crofton, ― Silane Oxidation Behind Reflected Shock Waves, Shock waves, Springer, Berlin, pp. 585–590. 2005

[3] M. Swihart, S. Girshick, Chem. Phys. Lett. 307 pg. 527–532., 1999.

[4] M. Swihart, S. Girshick, J. Phys. Chem. B 103, pg. 64–76, 1999.

[5] National *Institute for Occupational Safety and Health, NIOSH Pocket Guide to Chemical Hazards, Technical Report, Department of Health and Human Services,* 2005.

[6] M. Wooldridge, Prog. Energy Combust. Sci. 24, pg. 63–87, 1998.

[7] F. Tamanini, J. Chaffe, R. Jambar, Process Saf. Prog. 17, pg. 243–258, 1998.

[8] S.P.M. Bane, R. Mével, S.A. Coronel, J.E. Shepherd, Int. J. Hydrogen Energy 36, pg. 10107–10116, 2011.

[9] L. Zhang, H. Ma, Z. Shen, L. Wang, R. Liu, J. Pan, Exp. Therm. Fluid Sci. 102, pg.52–60, 2019.

[10] R. Mével, K.P. Chatelain, S. Lapointe, D.A. Lacoste, M. Idir, G. Dupree, N. Chaumeix, Combust. Flame 221, pg.150–159, 2020.

[11] International Agency for Research on Cancer, Some aromatic amines, hydrazine, and related substances, n-nitroso compounds and miscellaneous alkylating agents, evaluation of the cancerogenic risk of chemicals to man, Lyon: WHO, 1974.

[12] Gordon, S., McBride, B. J., Computer Program for Calculation of Complex Chemical Equilibrium Compositions and Applications – II. User's Manual and Program Description, NASA Ref Publ., No. 1311, 1996.

[13] Romeo, L., Torre, L., Pasini, A., Cervone, A., d'Agostino – Performance of different catalysts supported on alumina spheres for hydrogen peroxide decomposition, 43rd AIAA/ASME/SAE/ASEE Joint Propulsion Conference & Exhibit Cincinnati, OH, 2007.

[14] Rusek, J. J., ― New decomposition catalysts and characterization techniques for rocket-grade hydrogen peroxide, Journal of Propulsion and Power, Vol.12 (3), pp. 574-579, 1996.

[15] Romeo, L., Torre, L., Pasini, A., Cervone, A., d'Agostino, L., – Performance of different catalysts supported on alumina spheres for hydrogen peroxide decomposition, 43rd AIAA/ASME/SAE/ASEE Joint Propulsion Conference & Exhibit Cincinnati., 2007.

[16] Wernimont, E. J., Ventura, M., Grubelich, M. C., Vaughn, M. R., Escapule, W. R., ― Low-temperature start & operation capability of 82% hydrogen peroxide gas generators, 5th International Space Propulsion Conference, Heraklion, 2008.

[17] A. Konnov, (2005), ― Detailed reaction mechanism for small hydrocarbons combustion.

[18] Marshall, W. M., Deans, M. C., – Recommended figures of merit for green monopropellants,41st AIAA/ASME/SAE/ASEE Joint Propulsion Conference & Exhibit, San Jose, 2013.

[19] Kimball, R. F., ― The mutagenicity of hydrazine and some of its derivatives. Mutation

Research/Reviews in Genetic Toxicology 2, Vol. 39, pp. 111-126, 1977.

[20] Sotaniemi, E., Hirvonen, J., Isomaki, H., Takkunen, J., Kaila, J., Hydrazine toxicity in the human. Report of the fatal case, Ann. Clin. Res. 3, pp. 30-33, 1971.